



Title	Spatial mode compensation technique using progressive phase conjugation
Author(s)	Shen, Zeyu; Okamoto, Atsushi; Zhang, Shuanglu; Tomita, Akihisa
Citation	Optical review, 29(5), 440-449 https://doi.org/10.1007/s10043-022-00758-9
Issue Date	2022-10
Doc URL	http://hdl.handle.net/2115/90363
Rights	This version of the article has been accepted for publication, after peer review (when applicable) and is subject to Springer Nature 's AM terms of use, but is not the Version of Record and does not reflect post-acceptance improvements, or any corrections. The Version of Record is available online at: http://dx.doi.org/10.1007/s10043-022-00758-9
Type	article (author version)
File Information	OR_shen_final.pdf



[Instructions for use](#)

Spatial mode compensation technique using Progressive Phase Conjugation

Zeyu Shen^{1*}, Atsushi Okamoto¹, Shuanglu Zhang¹, Akihisa Tomita¹

¹*Graduate School of Information Science and Technology, Hokkaido University, Sapporo, Hokkaido 060-0814, Japan*

*E-mail: shen@optnet.ist.hokudai.ac.jp

We propose a spatial mode compensation method using progressive phase conjugation (PPC) to establish a dynamic control technology for mode distribution in multi-mode fiber (MMF). PPC is a phase conjugate generation technology that can be far away from the signal source and does not require an additional reference beam. We confirm the basic operation of the proposed scheme by considering the coupling efficiency between the compensated spatial mode component and incident mode. We quantitatively evaluate the mode recovery from the mixed state of LP11, LP22, LP02, and LP31 to LP01, the fundamental mode. By using a random optical diffuser to uniformly scatter the intensity distribution of the signal beam, high compensation performance can be obtained because the influence of the mode intensity distribution is reduced.

Keywords: mode-division multiplexing, multi-mode fibers, phase conjugation, mode compensation

1. Introduction

In recent years, the transmission capacity of single-mode fibers (SMFs) has reached its theoretical limit owing to the nonlinear Shannon effects and fiber fuse phenomenon [1–3]. The capacity constraints must be overcome to support future transmission demands. Optical transmission systems using few-mode fibers (FMFs), a type of multimode fiber (MMF), have been investigated [4, 5] to solve this issue. In FMFs, light can be transmitted in various modes, because the condition of light emission at the input end of the fiber determines the mode of light propagation. In the recently studied mode-division multiplexing (MDM) communication method, the transmission capacity of MMFs is theoretically proportional to the number of spatial modes, as each spatial mode is treated as a separate transmission channel light. Therefore, MDM systems with MMFs have both potentially high transmission capacity and high speed [6, 7]. However, imperfections in the fiber, such as uneven refractive index, core eccentricity and ellipticity, and bends, introduce coupling between light waves propagating in the MMF. The effect of superimposition between multiple modes with different propagation constants is known as mode coupling, which causes significant crosstalk during signal detection and results in a lower transmission rate. Therefore, the current MDM communication system requires large-scale multi-input multi-output (MIMO) signal processing after receiving optical signals, which is one of the obstacles for practical use [8, 9]. To reduce MIMO signal processing, various mode control techniques, such as mode compensation and mode conversion in the optical domain, are expected to be developed in the future.

In contrast, MMFs have conventionally been used for short-distance communication. Recently, from the optical interconnection viewpoint, MMFs have garnered attention because of their low cost and easy fiber-to-fiber connection [10, 11]. One method to speed up communication using MMFs is a single-mode excitation, which is an attempt to achieve high-speed communication by exciting only one mode in the MMF to avoid the effects of mode dispersion. However, as demonstrated in the development of the MDM systems described above, single-mode excitation results in many inter-mode couplings, even when FMFs are used. To solve these problems, adaptive optics have been investigated, in which spatial light modulators (SLMs) are placed at the excitation end of the fiber, and feedback is applied to reduce the mode dispersion at the receiver end [12, 13]. A multiplexed communication system that extends this technique has also been proposed [14]. However, the practical problem with this adaptive method is that a separate signal path from the receiving end to the transmitting end is required to control the mode distribution at the receiving end by optimizing the excitation profile at the transmitting end.

In this paper, to establish a dynamic control technology for mode distribution in MMFs, we propose a spatial mode compensation method using progressive phase conjugation (PPC). The PPC system was installed at the receiving end, where the spatial phase of the optical signal was measured by digital holography and mode compensation was performed using SLM based on the data. In PPC, the holographic reference light is generated by applying a spatial filter to a part of the signal light. The difference between our proposed method and the adaptive optical system described above is that in our method, mode compensation is performed at the receiving end rather than at the transmitting end, eliminating the need for communication channels other than fiber communication channels. Another advantage of our method is that the computational complexity is much smaller than that of conventional methods using Monte Carlo or other techniques because the optimal solution of mode compensation is calculated based on phase conjugation [15].

To confirm the basic operation of the proposed method, we performed a numerical simulation to restore the original linearly polarized (LP) mode of LP₀₁ from the mixed modes of LP₀₁ and LP₂₁. Subsequently, the influence of the diffusion channel on the mode compensation effect of PPC is discussed by changing the mixing component ratio of the higher-order modes. The specific goal of this study is to quantitatively evaluate the extent to which higher-order modes are reconstructed into fundamental modes by PPC. Furthermore, we demonstrate the effect of adding random diffusion to the signal before compensation on the compensation effect of PPC. The simulation results show that the proposed method can effectively compensate for the modal dispersion caused by the spatial mode beam transmission in the MMF, and the compensation performance is significantly improved using a random optical diffuser.

2. Principle of operation

Figure 1 shows the conceptual model of mode compensation when the fundamental mode is transmitted in an MMF using PPC technology. In general, a light wave propagating through the MMF is dispersed because of the superposition of multiple modes caused by mode coupling. As shown in Figure 1(a), a single pulse of the fundamental mode was injected into the MMF, but the pulse width increased at the output end of the MMF. As shown in Figure 1(b), the wavefront distortion is compensated by the PPC technology at the relay point, and the mode component of the light wave is restored to only the fundamental mode. As a whole, we can expect

a reduction in mode dispersion by keeping the higher-order mode components low. Recently, mode group diversity multiplexing (MGDM) has been studied, in which multiple spatial modes in an MMF are multiplexed and transmitted as a mode group, and the method using PPC may be applied to relay systems to improve the performance of MGDM [16, 17].

Figure 2 shows a schematic of the spatial mode beam compensation technique using the PPC technology. The compensation process was divided into three stages: phase measurement, conjugated phase generation, and mode compensation. The signal beam O before the fundamental mode enters the MMF for transmission is denoted by

$$O = A(x, y) \exp[i(kz - \omega t)], \quad (1)$$

where $A(x, y)$ is the amplitude of the signal beam and k is the wave number. Owing to the influence of the refractive index fluctuation and axial offset of the MMF, when the signal beam is emitted from the MMF, a phase distribution $\varphi(x, y)$ and amplitude distortion $A'(x, y)$ are generated. The received signal beam is defined as O' and is expressed as

$$O' = A'(x, y) \exp[i(kz - \omega t + \varphi(x, y))], \quad (2)$$

In the phase measurement process, the signal beam O' is divided into two optical paths by the beam splitter: the signal beam path and reference beam path. In the reference beam path, the plane-wave component was extracted from the signal beam through a low-pass spatial filter. The extracted plane wave has a high coherence with the signal beam, and because it is a plane wave, it satisfies the requirements for the reference beam in the phase measurement. Therefore, the extracted plane wave can be used as an internal reference beam. The phase measurement method is not limited by the PPC technology; however, to realize a high-performance PPC system, high-speed phase detection technology is required. In our research, holographic diversity interferometry (HDI) was used as the phase-detection technology [18, 19].

The signal beam and generated internal reference beam utilize the interference effects of the combination of a half mirror and polarizer to reconstruct the interference fringes required for the signal in a single measurement. Two interferograms were simultaneously obtained on two imagers, and the complex amplitude value of the signal beam was calculated using the two-channel algorithm developed by HDI to obtain the phase distribution $\varphi(x, y)$ of the signal beam. This calculation process is simple and can be completed in a short time. In the conjugated phase generation process, the sign of the detected phase distribution $\varphi(x, y)$ was reversed through computer operations to obtain the phase conjugate distribution $-\varphi(x, y)$. In the mode compensation process, the calculated phase conjugate distribution $-\varphi(x, y)$ of the spatial mode is displayed on the SLM. When the diffracted signal beam emitted from the MMF is modulated by the SLM, the phase distribution of the diffracted signal beam is converted by multiplying the original phase distribution by the phase conjugate distribution displayed on the SLM. It can be expressed as follows:

$$O = A'(x, y) \exp[i(kz - \omega t + \varphi(x, y))] \times \exp[i(-\varphi(x, y))]. \quad (3)$$

In Eq. (3), the wavefront distortion is canceled by the principle of phase compensation and is output as a plane wave. Because the fundamental mode LP01 itself has no phase distribution across the plane transversal to the propagation direction, eliminating the phase enables the spatial mode beam modulated by the SLM to be restored to the ideal fundamental mode. When the amplitude distortion is not sufficiently large, we can consider $\mathbf{A}' \approx \mathbf{A}$, ignoring the influence of the amplitude distortion. Accordingly, the output field of the spatial mode beam from the MMF distorted by mode couplings during propagation can be compensated through the PPC process. In this method, even if the spatial mode is distorted owing to fiber bending, the phase distribution including the distortion can be measured by the phase detector in real time, and the phase conjugate distribution displayed on the SLM changes in time; therefore, the mode fluctuation can be adaptively compensated. The response speed of the system depends on the response speed of the photodetector and SLM, as well as the time required to calculate the phase from the detection. In practical applications, the response speed needs to be shorter than the fluctuation time of the mode distribution induced by the changes in the fiber laying environment, such as temperature. However, the phase conjugate distribution is always displayed on the SLM and the compensation of PPC is continuous. Thus, even if the mode distribution fluctuates, it does not cause the transient signal to miss compensation. In the event of rapid changes in the installation environment of the fiber, such as the ambient temperature, the measurement speed struggles to keep up with the mode fluctuation, potentially reducing the transient compensation accuracy. To prevent communication rate degradation due to

such causes, there are, for example, MIMO processing methods after optical signal detection in MDM communication. In a real system, we aim to reduce its environmental impact by combining mode compensation in the optical domain with electronic processing after optical detection.

3. Numerical simulation

3.1 Simulation model

To verify the basic operation of the proposed scheme, we performed a numerical simulation to model the mode compensation of the PPC technology. The simulation parameters are listed in Table 1. The models and simulation flow are shown in Figure 3.

Table 1. Simulation Parameters

Common parameters			
Wavelength of laser source, (nm)	1550	Gray level of SLM	256
Zero-padding rate	2	Core diameter, (μm)	50
Number of SLM pixel	256×256	Collimated beam diameter, (μm)	80
Pitch of SLM pixel, (μm)	1.0	Pinhole diameter, (μm)	Variable
Numerical aperture of fiber	0.22	FFT focal length of low pass filter, (mm)	300
Diffusion angle by diffuser, (degree)	0.8	FFT focal length of diffuser, (mm)	150

The simulation process was divided into two parts: the distortion information measurement process and phase compensation process. We assume that the fundamental mode LP01 is converted into a superimposed mode of LP01 and higher-order LP modes, as the mode distribution is distorted by fiber transmission. This phenomenon can easily be caused by the mode coupling within the MMF. We used two fast Fourier transforms (FFT) and a small circular window to simulate a low-pass spatial filter for the $4f$ -system consisting of two lenses and a pinhole. The spatial mode beam was passed through this low-pass spatial filter and the component of a single plane wave in this part was extracted as the internal reference beam. Next, 90° was added to the phase to obtain two internal reference beams, which facilitated the calculation of the complex amplitude of the beam in the HDI method. Subsequently, two corresponding interferograms can be obtained by superimposing with the dispersed spatial mode beam and two internal reference beams. The phase distribution of the signal beam is calculated from the two interferograms using the two-channel algorithm developed by HDI method. In the phase compensation process, we inverted the sign of the observed phase distribution to obtain the conjugate phase distribution. This conjugate phase distribution is then multiplied by the dispersed spatial mode beam and then subjected to a FFT, which eliminates the phase distortion. This process simulates irradiating a dispersed spatial mode beam onto the SLM. The dispersed spatial mode beam was compensated and restored to the ideal fundamental mode LP01.

We evaluated the compensation accuracy by calculating the coupling efficiency (CE) between the complex amplitude of the post-compensation spatial mode beam and the complex amplitude of the desired ideal mode [20]. CE is calculated by expanding the field distribution on the desired ideal mode E_{id} with field profiles of the post-compensation spatial mode beam E and by taking the absolute square of the coefficient for the mode to be excited and is given by

$$CE = \left| \iint E^*(x, y) E_{id}(x, y) dx dy \right|^2, \quad (4)$$

where $*$ denotes complex conjugation.

3.2 Simulation results and discussions

Herein, we mixed the fundamental mode LP01 and the higher-order mode LP21 of different powers and changed their power mixing ratio to verify the mode compensation effect, where the ratio represents the ratio of the fundamental mode power to total power, and the total power is the sum of the fundamental and higher-order mode powers. Figure 4 shows the proportion of LP01 contained in the post-compensation beam and the intensity of the spatial mode beam after compensation. The vertical axis represents the CE of the modes contained, and the horizontal axis represents the ratio of the mixed proportion of the fundamental mode. With a decrease in the mixed proportion of LP01 in the spatial mode beam, the proportion of LP01 in the post-compensation spatial mode beam also decreases, and the proportion of LP02 increases. Even if LP01 is not

included in the spatial mode beam entering the PPC system, PPC can still recover the beam containing 40% LP01. In particular, when 70% of LP01 was mixed, approximately 87% of LP01 was contained in the post-compensation spatial mode beam. Therefore, we confirmed through numerical calculations that the spatial mode can be effectively compensated by PPC technology. The fewer the fundamental modes mixed in, the worse is the mode compensation effect. The longer the transmission distance of the spatial mode in the MMF, the worse is the mode compensation effect of PPC technology.

The main difference between the PPC technique and the conventional digital optical phase conjugation (DOPC) technique lies in the source of the reference beam. As stated earlier in the PPC technique, it is essential to obtain a plane wave, which is extracted from the signal beam through a low-pass spatial filter, as an internal reference beam. Thus, the compensation effect of the PPC technique depends on the integrity of the internal reference beam obtained using the low-pass spatial filter. We simulated the compensation effects when the pinhole diameter of the spatial filter was set to 40, 80, 120, and 160 μm , and when the external reference beam was used. The simulation results of the CE when mixing 80%, 60%, 40%, and 20% LP01 are shown in Figure 5. It can be seen from the figure that when the signal beam contains few plane wave components, the pinhole diameter must be reduced. When the pinhole diameter was 40 μm , there was little difference between the integrity of the generated internal reference beam and the external reference beam. However, under this condition, the spatial filter significantly reduced the optical power of the extracted internal reference beam, which might be insufficient to allow the usage of internal reference beam to obtain interference fringes during phase measurement. In contrast, if the pinhole diameter is increased to obtain an internal reference beam with sufficient optical power, high-precision plane wave components cannot be obtained because the high-frequency components of the signal beam will remain in the internal reference beam. Thus, it can be concluded that the calculated insufficient phase distribution accuracy results in a reduced compensation effect. In the simulation, the influence of the optical power of the internal reference beam could not be reflected because the intensity was not considered while calculating the phase. However, a trade-off between optical power and wavefront accuracy is required in the actual experimental process. To realize this PPC system, methods to reduce noise in light detection include the use of high-sensitivity photodetectors, as well as adjusting the ratio of signal beam and reference beam using the beam splitter and optimizing the pinball size in the generation of internal reference beam.

In addition, the fundamental mode diffuses to all higher-order mode channels, not just LP21. Therefore, we need to discuss whether the mode compensation effect of the PPC technology for each channel will be different if the fundamental mode diffuses to the channels of different higher-order modes. We selected LP11a, LP11b, LP21a, LP21b, LP02, LP31a, and LP31b as the diffusion channels for different higher-order modes. We mixed the fundamental mode and various higher-order modes in the same way, then compensated the dispersed modes using the PPC system and calculated the CEs. The simulation results are shown in Figure 6; for LP11a and LP11b, LP21a and LP21b, and LP31a and LP31b, the compensation effects of a and b of the same mode are identical, because they are the mutually orthogonal degenerate modes induced by rotation of the LP mode. Hence, they are excluded from the figure. The vertical axis represents the CE of the fundamental mode, and the horizontal axis represents the ratio of the mixed fundamental mode. The four lines represent the four different mixed modes, among which the blue, orange, gray, and yellow lines represent LP01 mixed with LP11, LP21, LP02, and LP31 modes, respectively. When the fundamental mode was mixed with LP11, LP21, and LP31, the mode compensation effect was dramatically reduced as the proportion of higher-order modes increased. The compensation effect when the fundamental mode was mixed with LP31 was far lower than that when mixed with LP21. In particular, when 40% of LP01 and LP02 were mixed, LP01 could still be compensated to approximately 85%; when 40% of LP01 and LP11 were mixed, LP01 could only be compensated to approximately 68%. LP21 was only approximately 8 points lower than LP11, but when 40% of LP01 and LP31 were mixed, only approximately 45% of the compensated LP01 remained. From these results, it was found that the compensation effect of LP02 was the highest, followed by the compensation effect of LP11, LP21, and LP31. Therefore, with the exception of LP02, we found that the closer the diffusion channel is to the channel of the fundamental mode, the higher is the compensation effect. Furthermore, typically, the fundamental mode simultaneously diffuses into the channel of several higher-order modes and not just into one

higher-order mode; therefore, we mixed several higher-order modes with the fundamental mode. We simultaneously mixed the fundamental mode with two higher-order modes of the same proportions, as shown in Figure 7. The results show that PPC can compensate for mixed beams of several higher-order modes. However, when the mixed proportion of the higher-order spatial mode was greater than 50%, the compensation accuracy was lower than 70%. This means that the distance where PPC technology can adequately compensate for the spatial mode is very short, which does not meet our expectations. Thus, it is necessary to improve the compensation effect of the PPC technology for higher-order modes.

4. Improvement of compensation effect by diffuser

According to the intensity distribution of the various $LP_{l,m}$ modes, there is an intensity distribution in the central part when the variation in the intensity distribution in the azimuthal plane $l = 0$, and there is no intensity distribution in the central part when $l > 1$. The intensity distribution of the mode with a small l is closer to the center, and the intensity distribution of the mode with a large l is on the outer side. The higher the l order, the farther the mode intensity distribution is from the center, and the smaller the intensity overlap is with the fundamental mode. Because LP02 has an intensity distribution in the center, and the intensity overlap amount with the fundamental mode is greater than that of LP01, the compensation effect of LP02 is still better than that of LP11, even if the order of LP02 is higher than that of LP11. Therefore, the mode compensation effect of PPC technology depends on the intensity overlap between the higher-order and fundamental modes. Even if the phase of the spatial mode is compensated by PPC technology, it is difficult to restore the higher-order mode with no intensity distribution in the central part to the fundamental mode with the intensity concentrated in the central part. The poor compensation effect can be attributed to the excessive amplitude distortion $A'(x, y)$ in Eq. (3). At this time, the influence of amplitude distortion cannot be ignored. Therefore, we propose adding a random optical diffuser to eliminate this influence. As shown in Figure 8, we added a random phase diffuser and lens at the Fourier plane before the dispersed spatial mode beam entered the PPC system. In this method, the intensity distribution of the input spatial mode beam is diffused uniformly using a random optical diffuser and an optical lens. Regardless of the mode, if it passes through the diffuser, the intensity distribution is uniformly diffused over the entire plane, and the intensity of each place on the plane is equal. Even for a higher-order mode with no intensity distribution in the central part, there will be an intensity distribution in the central part after passing through the random optical diffuser, and the amount of intensity overlap with the fundamental mode will increase. Therefore, when the diffused spatial mode beam enters the PPC system again, the spatial mode beam can be more easily restored to the fundamental mode through PPC technology owing to the increased amount of intensity overlap. Furthermore, even after transmission through the random diffuser, the wavefront distortion is considerably reduced by allowing it to pass through the small pinhole, to ensure that the problem of inability to perform interferometric measurements due to reduced coherency does not arise. In addition, not only in this method, interference with a signal or reference beam using a random diffuser is often seen in the field of hologram memory and digital holograms [21, 22].

In the simulation, the diffused mode was calculated by extending the original mode over a wider region using a random optical diffuser at a diffusion ratio of N_{diff} [23]. The original mode comprises $N_{dx} \times N_{dy}$ SLM pixels, and the random optical diffuser comprises random phase distribution images of the imported $N_{dx}N_{diff} \times N_{dy}N_{diff}$ SLM pixels, where N_{dx} and N_{dy} are the number of SLM pixels along the x and y axes, respectively. The diffusion ratio N_{diff} is defined as the ratio of the sizes of the original and diffused modes, and is calculated as

$$N_{diff} = \frac{\theta_d + \tan^{-1}(N_{dx}L_{dx}/2L_f)}{\tan^{-1}(N_{dx}L_{dx}/2L_f)}, \quad (5)$$

where θ_d is the diffusion angle of the random optical diffuser, L_{dx} is the pitch of the SLM pixels, and L_f is the focal length of the Fourier transform lens.

The phase of the spatial mode beam was transformed by granting it a random phase distribution, and the complex amplitudes were subsequently collimated using FFT; the intensity of the spatial mode beam changes accordingly. Then, the proportion of the fundamental mode in the post-compensation spatial mode beam with a random optical diffuser was obtained by repeating the mode compensation process of the PPC technology. Figure 9 shows the simulation results. By comparing the two groups of data in the figure, for results with and without a random optical diffuser, the compensation effect can be greatly improved by using a random optical diffuser. In particular, when the higher-order mode occupies a relatively large amount in the spatial mode beam, the compensation effect can be significantly improved. When 60% of LP01 was mixed with various higher-

order modes, the compensation accuracy was approximately 90%. Even if LP01 was not included in the spatial mode beam, LP11 and LP21 could compensate for LP01 by approximately 90%, and LP02 and LP31 could compensate for LP01 by more than 74%. Compared with the case when the diffuser was not used, the CE of LP21 increased by 46 points, the CE of LP31 increased by 47 points, and the compensation accuracy of the higher-order mode was significantly improved. However, when the fundamental mode occupies a relatively large portion of the spatial mode beam, the mode compensation effect is reduced. When 90% of the LP01 was mixed with the higher-order mode, the LP01 could originally be compensated to approximately 98%; however, after adding the random optical diffuser, it could only be compensated to approximately 93%, and the compensation effect was reduced by approximately 5 points. This is because the intensity distribution of the central part diffuses to the surrounding area after the fundamental mode passes through a random optical diffuser. The intensity distribution of the central part is weaker than that without the random optical diffuser, and the intensity overlap with the ideal fundamental mode is also lower than that without the random optical diffuser; therefore, the compensation effect is worse. The longer the transmission distance, the more the signal power of the fundamental mode moves to a higher-order mode channel. Therefore, for long-distance transmission, the effect of mode correction can be greatly improved by adding a random optical diffuser.

5. Conclusions

We proposed a mode compensation method using PPC technology to reduce the mode dispersion generated when the spatial mode is transmitted in the MMF. The operation of mode compensation in the spatial mode using PPC technology was confirmed through numerical analysis. Furthermore, we discussed the influence of diffusion channels on the compensation effect. We found that the higher the intensity overlap between the diffused higher-order mode and fundamental mode, the higher is the compensation effect. To solve the problem of the poor compensation effect of higher-order modes, we also proposed a method to diffuse the intensity distribution through a random optical diffuser. Numerical analysis results showed that adding a random optical diffuser can significantly improve the compensation effect of the higher-order modes.

Acknowledgments

This work was supported by JST SPRING (grant number JPMJSP2119).

References

- [1] D. J. Richardson, *Science*, vol. 330, no. 6002, pp. 327–328, 2010, doi: [10.1126/science.1191708](https://doi.org/10.1126/science.1191708).
- [2] R. Essiambre, G. Kramer, P. J. Winzer, G. J. Foschini, B. Goebel, *J. Lightwave Technol.*, vol. 28, no. 4, pp. 662–701, 2010, doi: [10.1109/JLT.2009.2039464](https://doi.org/10.1109/JLT.2009.2039464).
- [3] R. J. Essiambre and R. W. Tkach, in *Proc. IEEE*, vol. 100, no. 5, pp. 1035–1055, 2012, doi: [10.1109/JPROC.2012.2182970](https://doi.org/10.1109/JPROC.2012.2182970).
- [4] P. Sillard, M. Bigot-Astruc, D. Boivin, H. Maerten, and L. Provost, in *37th European Conference and Exposition and Optical Communications*, 2011, doi: [10.1364/ecoc.2011.tu.5.lecervin.7](https://doi.org/10.1364/ecoc.2011.tu.5.lecervin.7).
- [5] P. Sillard, D. Molin, M. Bigot-Astruc, A. Amezcua-Correa, K. De Jongh, and F. Achten, in *Eur. Conference on Optical Communication, ECOC*, 2015, vol. p. 2015-Novem, doi: [10.1109/ECOC.2015.7341642](https://doi.org/10.1109/ECOC.2015.7341642).
- [6] D. Soma et al., *J. Light Technol.*, vol. 36, no. 6, pp. 1362–1368, 2018, doi: [10.1109/JLT.2018.2799380](https://doi.org/10.1109/JLT.2018.2799380).
- [7] S. Beppu et al., *J. Light Technol.*, vol. 38, no. 10, pp. 2834–2840, 2020, doi: [10.1109/JLT.2020.2979195](https://doi.org/10.1109/JLT.2020.2979195).
- [8] D. Soma et al., *J. Light Technol.*, vol. 36, no. 6, pp. 1375–1381, 2018.
- [9] T. Hayashi et al., *J. Lightwave Technol.*, vol. 35, no. 4, pp. 748–754, 2017, doi: [10.1109/JLT.2016.2617894](https://doi.org/10.1109/JLT.2016.2617894).
- [10] A. Wang, L. Zhu, L. Wang, J. Ai, S. Chen, and J. Wang, *Opt. Express*, vol. 26, no. 8, p. 10038–10047, 2018, doi: [10.1364/OE.26.010038](https://doi.org/10.1364/OE.26.010038).
- [11] M. U. Hadi, J. Nanni, O. Venard, G. Baudoin, J. L. Polleux, and G. Tartarini, *Radioengineering*, vol. 29, no. 1, pp. 37–43, 2020, doi: [10.13164/re.2020.0037](https://doi.org/10.13164/re.2020.0037).
- [12] R. A. Panicker, A. P. T. Lau, J. P. Wilde, and J. M. Kahn, *J. Lightwave Technol.*, vol. 27, no. 24, pp. 5783–5789, 2009, doi: [10.1109/JLT.2009.2036683](https://doi.org/10.1109/JLT.2009.2036683).
- [13] M. B. Shemirani, J. P. Wilde, and J. M. Kahn, *J. Lightwave Technol.*, vol. 28, no. 18, pp. 2627–2639, 2010, doi: [10.1109/JLT.2010.2058092](https://doi.org/10.1109/JLT.2010.2058092).
- [14] N. Sheffi, and D. Sadot, *J. Lightwave Technol.*, vol. 35, no. 11, pp. 2098–2108, 2017, doi: [10.1109/JLT.2017.2656238](https://doi.org/10.1109/JLT.2017.2656238).
- [15] B. Y. Zel'dovich, V. I. Popovichev, V. V. Ragul'skii, and F. S. Faizullov, in *Landmark Papers on Photorefractive Nonlinear Optics*, World Scientific, 1995, pp. 303–306.
- [16] K. Benyahya et al., *J. Lightwave Technol.*, vol. 36, no. 2, pp. 355–360, 2018, doi: [10.1109/JLT.2017.2779825](https://doi.org/10.1109/JLT.2017.2779825).
- [17] F. Feng et al., 2016, doi: [10.1364/ofc.2016.w3d.5](https://doi.org/10.1364/ofc.2016.w3d.5).
- [18] A. Okamoto, K. Kunori, M. Takabayashi, A. Tomita, and K. Sato, *Opt. Express*, vol. 19, no. 14, p. 13436–13444, 2011, doi: [10.1364/OE.19.013436](https://doi.org/10.1364/OE.19.013436).
- [19] Y. Goto, A. Okamoto, Y. Wakayama, K. Ogawa, J. Nozawa, A. Tomita, T. Tsuritani, *Opt. Express*, vol. 24, no. 21, p. 24739, Oct. 2016, doi: [10.1364/OE.24.024739](https://doi.org/10.1364/OE.24.024739).
- [20] T. Suhara, in *Comprehensive Microsystems*, Elsevier, 2008, pp. 165–199. doi: [10.1016/B978-044452190-3.00029-X](https://doi.org/10.1016/B978-044452190-3.00029-X).
- [21] K. Oe, T. Nomura, *Appl. Opt.* 57, 5652–5656 (2018), doi: [10.1364/AO.57.005652](https://doi.org/10.1364/AO.57.005652).
- [22] W. Lin, Li. Chen, S. Zhou, T. Yeh, W. Su, *Optical Engineering* 60(7), 075105 (26 July 2021), doi: [10.1117/1.OE.60.7.075105](https://doi.org/10.1117/1.OE.60.7.075105).
- [23] S. Zhang, A. Okamoto, T. Shiba, H. Hayashi, K. Ogawa, A. Tomita, T. Takahata, S. Shinada, Y. Goto, N. Wada, *Opt. Review*, vol. 28, no. 2, pp. 181–189, Apr. 2021, doi: [10.1007/s10043-021-00648-6](https://doi.org/10.1007/s10043-021-00648-6).

Figure Captions

Fig.1 (Color online) Conceptual model of mode compensation using PPC. (a) Mode dispersion is produced in MMF, (b) Compensate by PPC to reduce modal dispersion

Fig.2 (Color online) Schematic diagram of the spatial mode beam compensation technique using PPC

Fig.3 (Color online) Simulation models and flow. (a) Distortion information measurement process, (b) Phase compensation process

Fig.4 (Color online) CE vs. mixed LP01 ratio

Fig.5 (Color online) Pinhole diameter and compensation effect

Fig.6 (Color online) 4 modes of CE

Fig.7 (Color online) 2 higher-order modes mixed of CE

Fig.8 (Color online) Improved analytical model

Fig.9 (Color online) Simulation results with and without using random optical diffuser. (a) CE vs. mixed LP11 ratio, (b) CE vs. mixed LP21 ratio, (c) CE vs. mixed LP02 ratio, (d) CE vs. mixed LP31 ratio

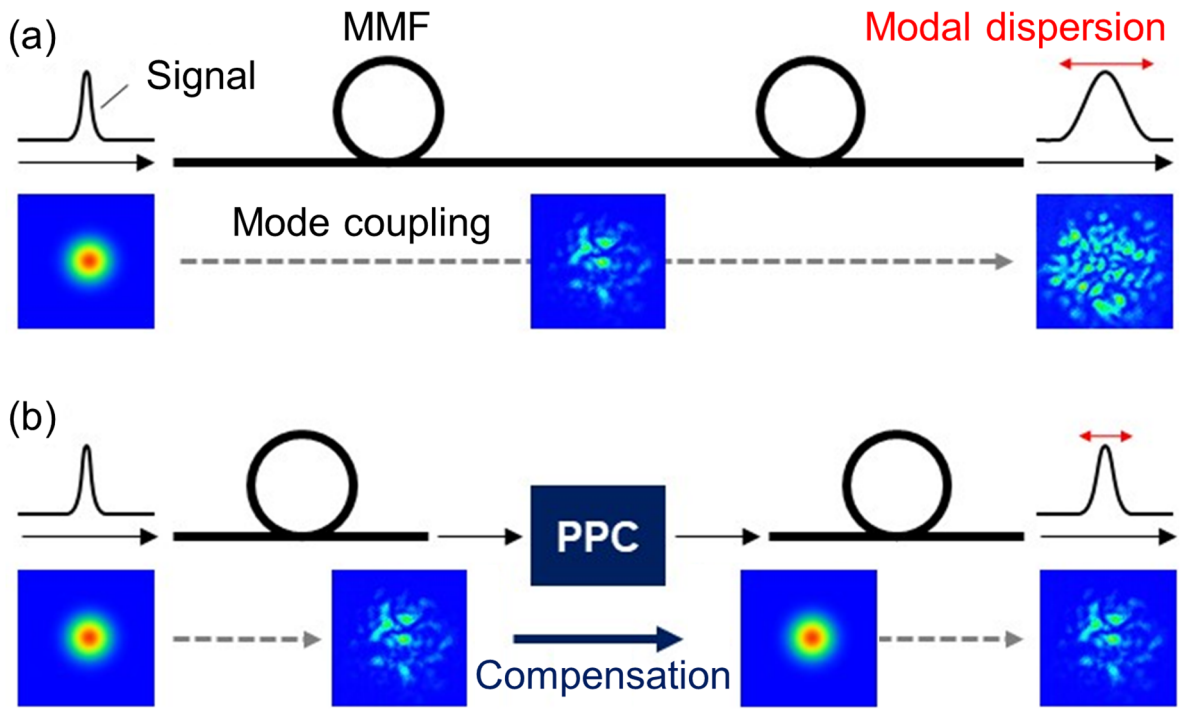


Fig.1 (Color online)

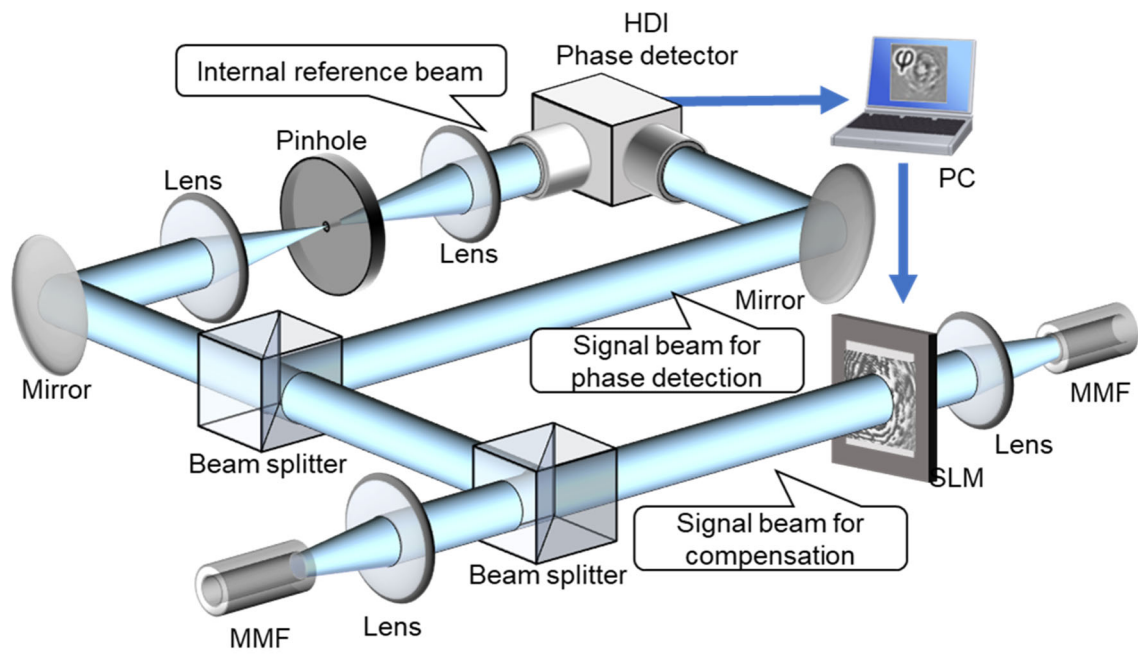


Fig.2 (Color online)

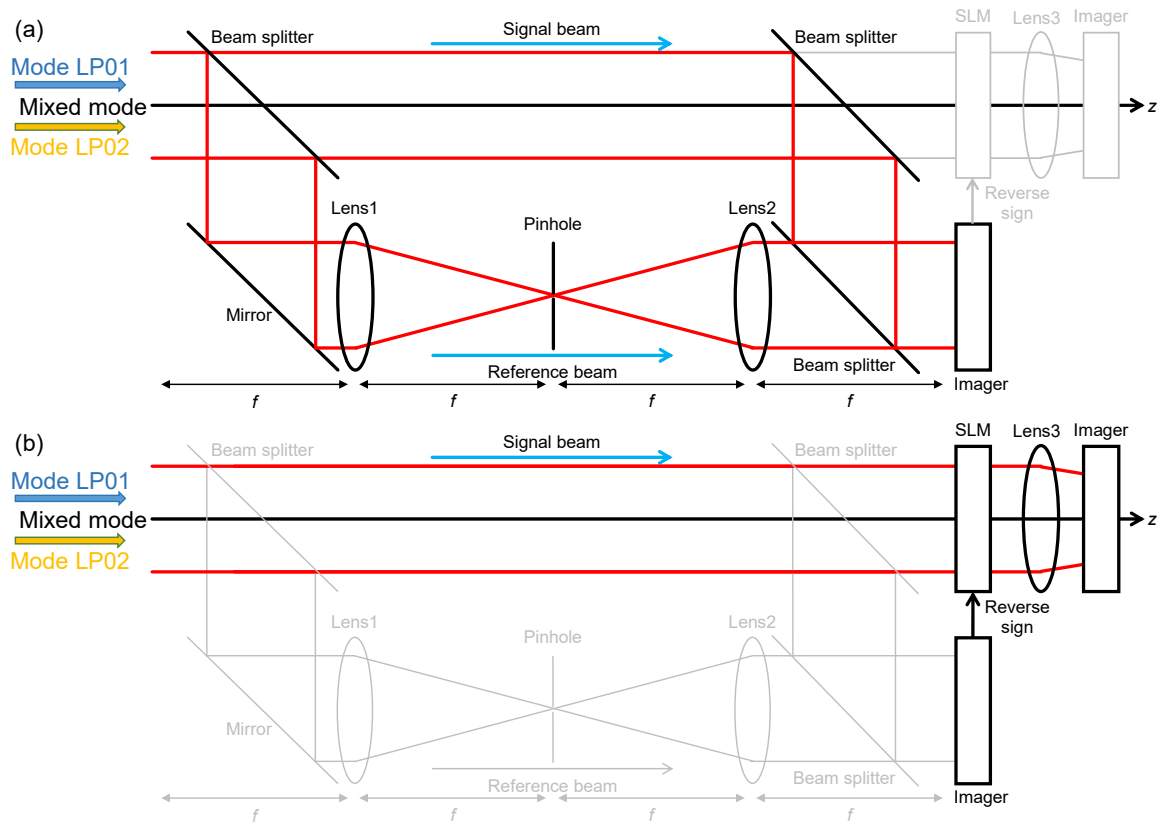


Fig.3 (Color online)

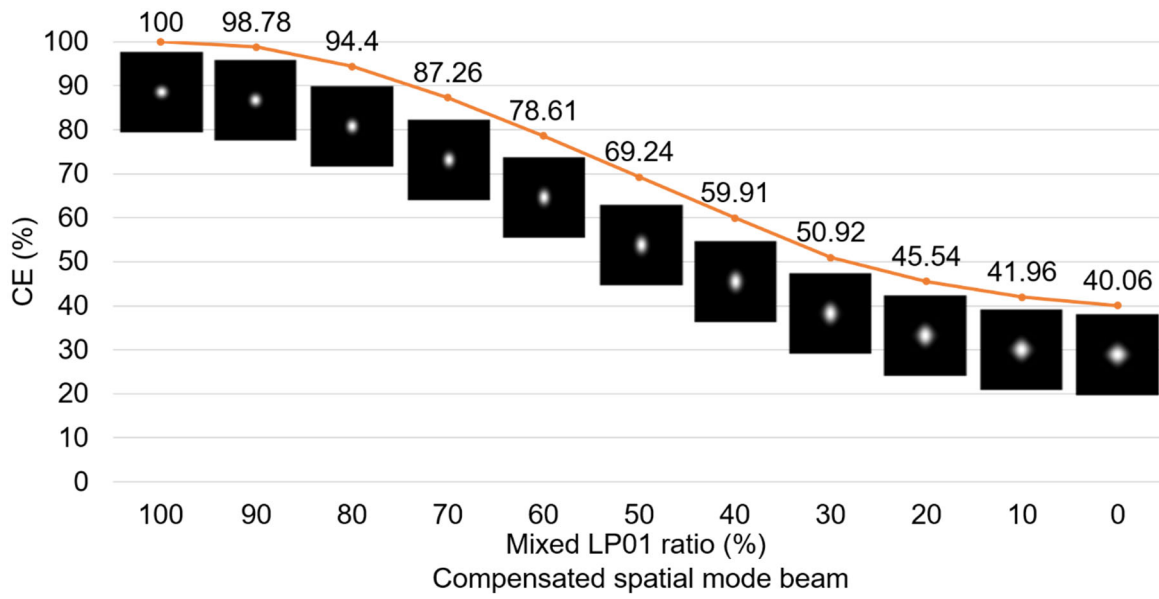


Fig.4 (Color online)

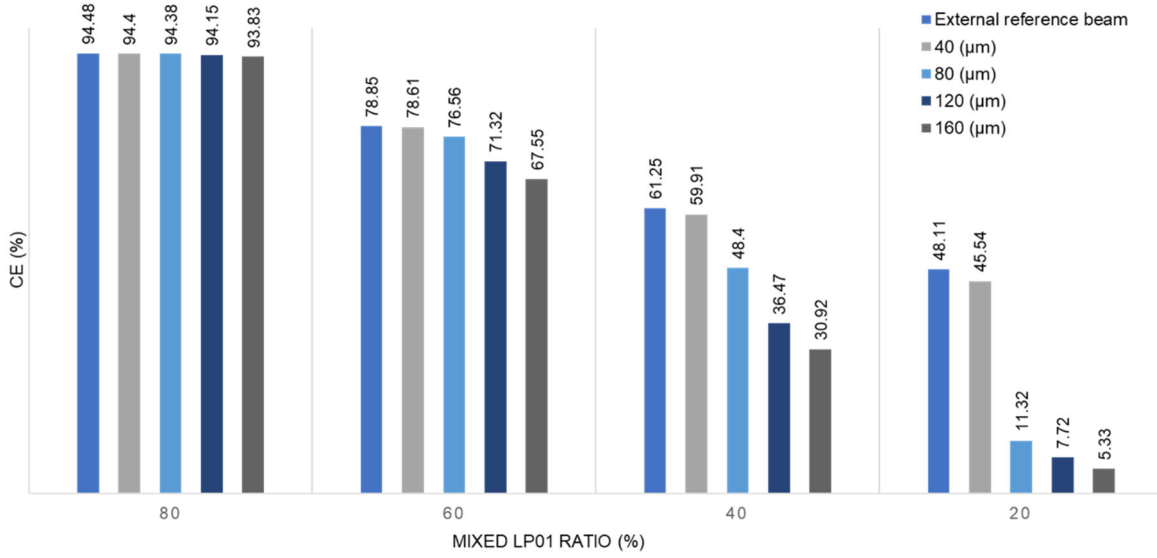


Fig.5 (Color online)

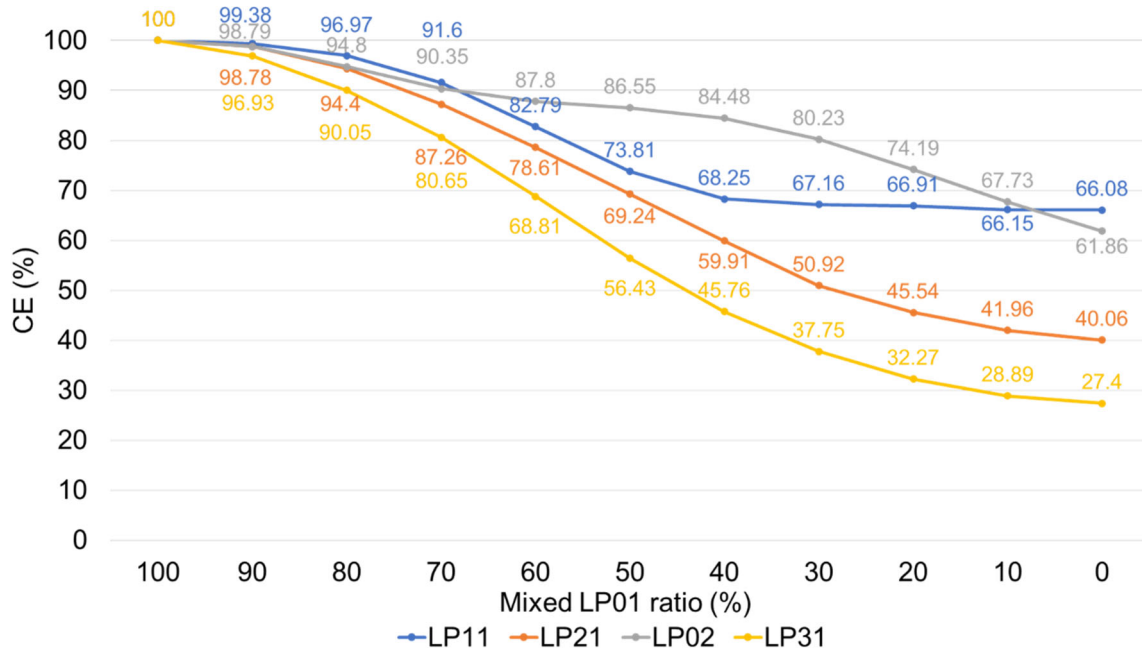


Fig.6 (Color online)

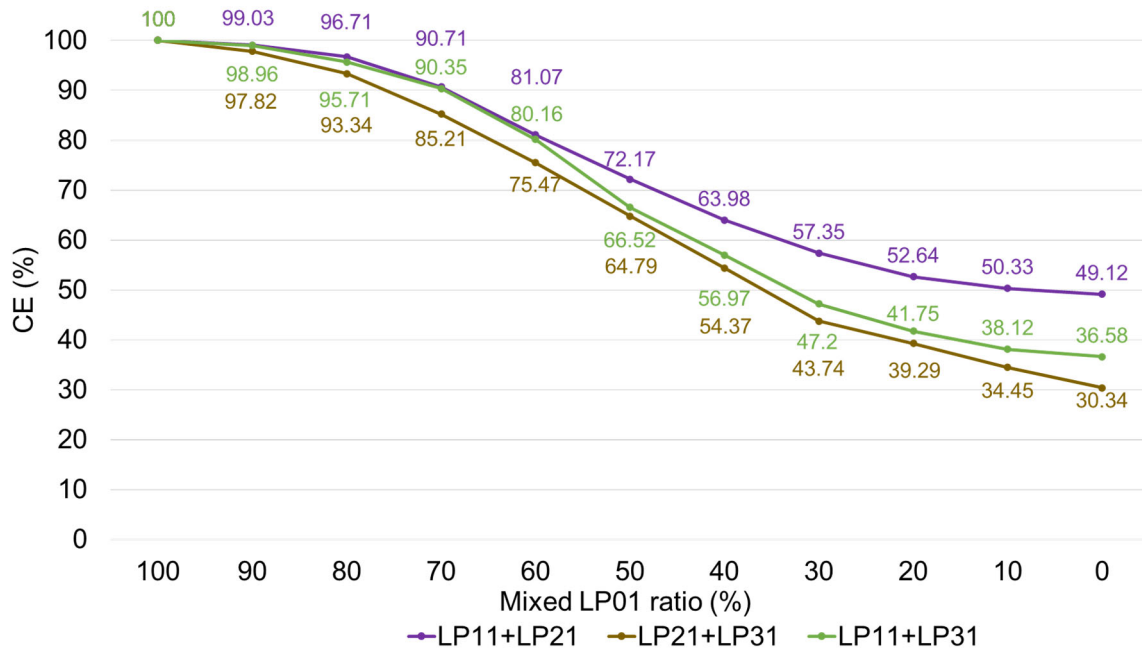


Fig.7 (Color online)

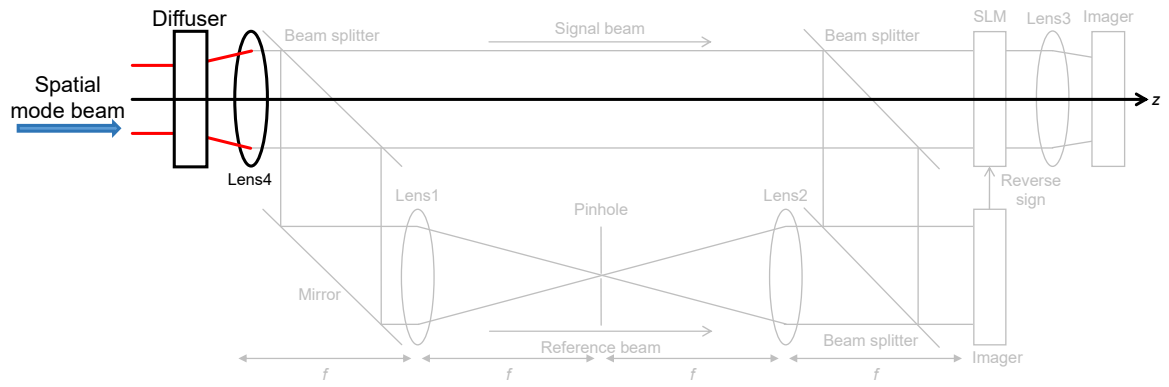


Fig.8 (Color online)

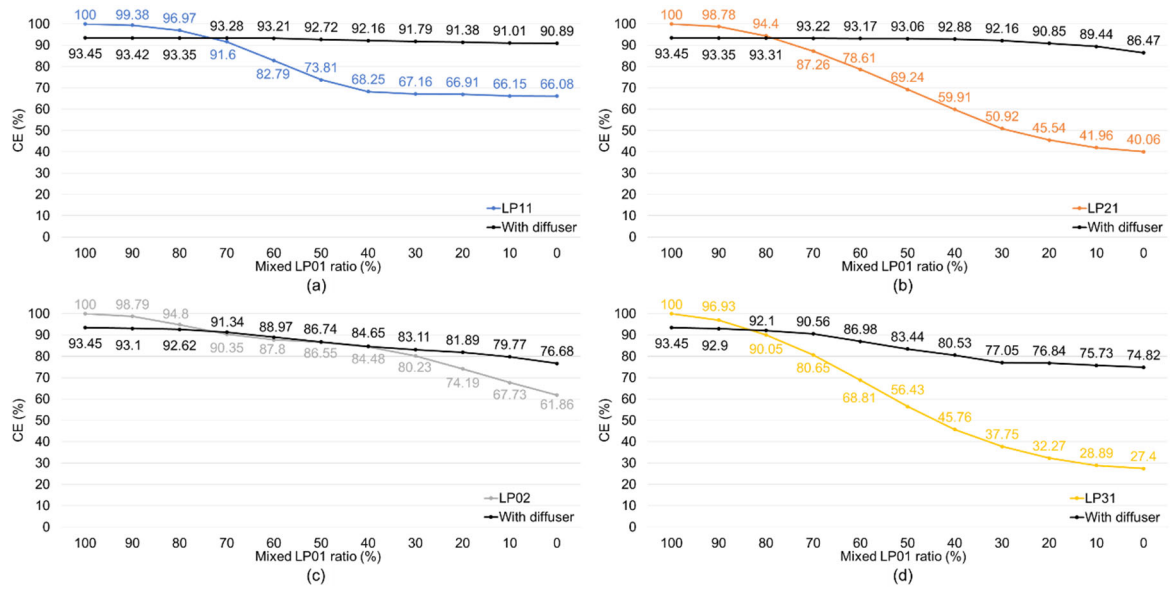


Fig.9 (Color online)